J Fluoresc (2008) 18:423–432
DOI 10.1007/s10895-007-0282-1

ORIGINAL PAPER

Interactions of Nile Blue with Micelles, Reverse Micelles and a Genomic DNA

Rajib Kumar Mitra · Sudarson Sekhar Sinha · Samir Kumar Pal

Received: 17 October 2007 / Accepted: 5 November 2007 / Published online: 7 December 2007

Abstract In this contribution we report studies on the nature of binding of a small ligand/drug Nile blue (NB) with sodium dodecyl sulfate (SDS) micelles, bis-(2-ethyl-ehexyl) sulfosuccinate (AOT)/isooctane reverse micelles (RM) and a genomic DNA extracted from Salmon sperm. With detailed steady state and picosecond resolved optical spectroscopic techniques, we examined the fluorescence quenching of the ligand upon complexation with the SDS monomers and DNA. Polarization analyzed picosecond-resolved fluorescence measurements reveal geometrical restriction on the probe in SDS micelles, AOT-RM and DNA. Steady state and time resolved studies on the probe in nanocages of AOT RM with various degrees of hydration (w_0) reveal the existence of NB as two distinct species namely, neutral and cationic. This study confirms that the emission of NB in aqueous micelles and DNA solution is due to the cationic form of the drug. Our experiments clearly identified non-specific electrostatic and intercalative modes of interaction of the probe with the DNA at lower and higher DNA concentrations respectively. The nature of binding of NB in presence of the DNA and SDS micelles reveals that the binding affinity of the probe is higher with the micelles than with the DNA. The complex rigidity of NB with DNA and its fluorescence quenching with DNA elucidate a strong recognition mechanism between NB and DNA.

R. K. Mitra · S. S. Sinha · S. K. Pal (✉)
Unit of Nano-Science and Technology, Department of Chemical, Biological & Macromolecular Sciences,
S.N. Bose National Centre for Basic Sciences,
JD Block, Sector III, Salt Lake,
Kolkata 700098, India
e-mail: skpal@bose.res.in

Keywords Nile blue · SDS micelles · AOT Reverse micelle · DNA intercalation · Fluorescence quenching · Picosecond resolved fluorescence anisotropy

Introduction

Nile blue (NB) is a well known DNA binding probe [1]. This probe is a member of the benzophenoxazine class of dyes, which has been found to be localized selectively in animal tumors [2]. These kinds of dyes exhibit relatively low systemic toxicity and some of them retard tumor growth [3, 4]. The planar hydrophobic phenoxazine moiety of NB is expected to facilitate the intercalation of NB into relatively non-polar interior of DNA helix. Compared to the other conventional intercalators, the use of NB has a merit of having low toxicity and comparable sensitivity for DNA quantification [1]. Despite the general utility of NB as a DNA probe, only limited reports on the interaction of this dye with biomimicking self-assembled systems, like micelles, reverse micelles (RMs) and DNA are available in the literature [1, 5–10]. Das et al. [9] reported the presence of the deprotonated form of NB in neat Triton X-100 (TX-100)/benzene-hexane solution and with addition of water as the hydration of RM increased the protonated form of NB appeared. Hong et al. [10] studied the interaction of NB on the surface of sodium dodecylbenzenesulfonate (SDBS) micelles. They found that the aggregation of the dye on the micellar surface obeyed the Langmuir adsorption isotherm. The studies of the dye with DNA conclude that NB serves as an intercalator to the stacked base pairs of nucleic acids. Electrochemical studies by Ju et al. [6] on the interaction of NB with DNA on gold electrodes concluded that the binding of NB with DNA in solution contains both electrostatic and intercalative inter-

actions, and also suggested that NB can be used as an electrochemical indicator for preparation of DNA sensors. Yang et al. [8] suggested that the intercalation between NB and DNA can be utilized to use NB as a visible dye for DNA detection in electrophoresis gel. The steady-state and ultrafast time-resolved spectroscopic studies of NB in homogeneous solvents confirm an ultrafast intermolecular electron/proton transfer process in diffusionless electron-donating [11] and hydrogen-bond acceptor [12–14] solvents respectively. The former process occurs within 100fs, whereas the later within a few ps. The dye exhibits very short excited-state lifetime in water (0.38ns) with respect to a few nanosecond excited-state lifetime in aprotic solvents [15].

The photophysics of NB in pure solvents is well characterized in literature. However, its interaction with microheterogeneous systems (e.g. micelles, RMs, DNA etc.) is only discretely studied so far. A complete study on the interaction of this dye with biomimicking systems and DNA is strongly demanding and we initiate a series of photophysical studies on the interaction of NB with bio-mimicking self-organized systems like micelles, RMs and DNA. In this paper we report absorption, emission, picosecond-resolved fluorescence, rotational fluorescence anisotropy of NB molecules in SDS micelles, AOT/isooctane RMs and in a genomic DNA extracted from salmon sperm (SS-DNA). The polarization analyzed fluorescence anisotropy for the micelles-NB, RM-NB and DNA-NB complexes elucidate the binding rigidity of the probe NB. The nature of DNA-binding of the probe NB in presence of SDS micelles is also explored in our studies. The structural integrity of the DNA in presence of SDS micelles has been confirmed by circular dichroism (CD) spectroscopic studies. Such a comprehensive study of the photophysics on NB in DNA and mimicking restricted systems is important to exploit this nontoxic fluorescent dye as a tool for DNA-recognition in biologically relevant macromolecular microenvironment.

Materials and methods

The fluorescent probe Nile blue (NB; Scheme 1) chloride was obtained from Sigma. Sodium dodecyl sulfate (SDS) and cetyltrimethyl ammonium bromide (CTAB) were products of Fluka. Salmon sperm DNA (SS-DNA), bis-(2-ethylehexyl) sulfosuccinate (AOT) and Triton X-100 (TX-100) were purchased from Sigma-Aldrich and used without further purification. Isooctane (i-Oc) was a product of Spectrochem. Aqueous micelles were prepared by adding calculated amounts of surfactant in known volume of double-distilled water and stirring for about 45min. The RMs containing the probe of different w_0 (=[water]/[AOT])

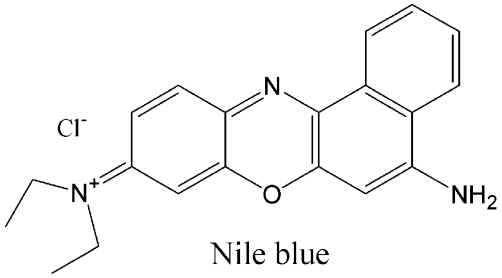

Scheme 1 Molecular structure of the fluorescence probe NB

values were prepared by injecting known amount of aqueous probe solution into measured volume of AOT-isooctane solution ([AOT] = 100mM) followed by stirring to obtain a clear solution. The nucleotide concentrations of the DNA samples were measured by absorption spectroscopy using the average excitation coefficient of nucleotide ($6{,}600 M^{-1}$ cm^{-1} at 260nm) [16] and considered to be the concentrations of the DNAs. The initial concentration of the probe was fixed at 2μM in all the solutions in order to avoid self-aggregation.

Steady state absorption and emission were measured with Shimadzu UV-2450 spectrophotometer and Jobin Yvon Fluoromax-3 fluorimeter respectively. Circular dichroism (CD) spectra were taken in a Jasco-815 spectrometer using a quartz cell of path length of 1cm. All fluorescence decays were taken by using picosecond-resolved time correlated single photon counting (TCSPC) technique. The commercially available setup is a picosecond diode laser pumped time resolved fluorescence spectrophotometer from Edinburgh Instrument, UK. It has an instrument response function (IRF) of 80ps. The picosecond excitation pulse from Picoquant diode laser was used at either 633nm or 409nm. The observed fluorescence transients are fitted by using a nonlinear least square fitting procedure to a function $\left(X(t) = \int_0^t E(t')R(t-t')dt'\right)$ comprising of convolution of the IRF ($E(t)$) with a sum of exponentials $\left(R(t) = A + \sum_{i=1}^{N} B_i e^{-t/\tau_i}\right)$ with pre-exponential factors (B_i), characteristic lifetimes (τ_i) and a background (A). Relative concentration in a multi-exponential decay is finally expressed as; $a_n = \frac{B_n}{\sum_{i=1}^{N} B_i}$. The quality of the curve fitting is evaluated by reduced chi-square and residual data. The details of the time-resolved measurements and construction of time resolved emission spectra (TRES) have been described in our earlier studies [17]. To ascertain the types of species present in the AOT/isooctane reverse micelles, we adopted the time resolved area normalized emission spectra (TRANES) technique developed by Periasamy's group [18–20]. TRANES is a model free modified version of TRES. A useful feature of this method is that presence of an isoemissive point in the spectra indicates the presence of two emitting species, which are kinetically coupled either irreversibly or reversibly or not coupled at all. For anisotropy measurements, emission

polarization was adjusted to be parallel or perpendicular to that of the excitation and anisotropy is defined as,

$$r(t) = \frac{I_{\parallel} - G.I_{\perp}}{I_{\parallel} + 2.G.I_{\perp}}$$

The magnitude of G, the grating factor was determined by using a NB solution in water following longtime tail matching technique [21].

Results and discussion

Absorption and emission spectra of the probe NB upon interaction with SDS of various concentrations are shown in Fig. 1a. As observed from the figure, NB produces an absorption maximum at 635nm in water, which is blue shifted to 590nm in presence of 3.5mM SDS. The appearance of a new peak in the spectrum indicates the formation of a complex of the dye with surfactant monomers [22, 23]. Sarkar et al. [22] earlier reported such an interaction between a cationic dye, crystal violet and SDS, resulting in the formation of a shoulder in the blue region of the absorption spectrum. Such an interaction might also lead to the formation of dimers of the dye. At a higher SDS concentration (6mM), two absorption peaks appear; one at 595nm and the other at 635nm. The absorption peak at the blue end is weakened when SDS concentration is further increased to 7mM, at the expense of the enhancement of the 635nm peak. The peak at 595nm vanishes at 8mM SDS (critical micellar concentration, cmc of SDS), revealing only a single peak at 636nm, with higher absorbance than that of the aqueous solution. The corresponding fluorescence spectra (inset of Fig. 1a) display no considerable shift of the peak position [~674nm in pure water] at [SDS]<cmc with respect to that in bulk water, however, the intensity decreases gradually. At the cmc a ~3–4nm blue shift occurs with a huge increase in the intensity. The fluorescence intensities at the peaks of the emission spectra have been plotted against concentration of SDS in Fig. 1b. At [SDS]<cmc, intensity decreases indicating a significant quenching. However, as the concentration of SDS crosses its cmc, the intensity sharply increases by almost two orders of magnitude. A Stern-Volmer equation, $\frac{I_0}{I} = 1 + K_{SV}[SDS]$, (where, I_0 and I are the fluorescence intensities in absence and presence of quencher (SDS) and K_{SV} is the formation constant of the quenching complex) is fitted in the quenching regime (inset of Fig. 1b). A good linear fit is obtained with a corresponding quenching constant (K_{SV}) of 1.3 × 10^4l mol^{-1}. An alternate form of the Stern–Volmer equation can be expressed in tems of the excited-state lifetime, $\frac{\tau_0}{\tau} = 1 + K_{SV}[SDS]$, where τ_0 is the excited-state lifetime of the probe in absence of the quencher and τ is that in presence of the quencher. The change of (τ_0/τ) does not match with that of intensity (I_0/I) confirming the static nature of the quenching [24]. The quenching of NB fluorescence by SDS below its cmc might have been caused due to the formation of dye-surfactant ion-pairs (as evidenced from the absorption spectra), which progressively associate to form an aggregated type of structure [22, 23]. We perform the same experiment with a cationic surfactant cetyl trimethylammonium bromide (CTAB) and a nonionic surfactant, TX-100 and found no quenching of NB fluorescence, which supports the interpretation of the ion-pair formation between the positively charged dye and the negatively charged surfactant monomers. With increase in SDS concentration, intensity increases sharply and reaches a constant value beyond the cmc of SDS. The increase in the fluorescence intensity of NB in SDS solution above cmc can be rationalized as follows. At [SDS]≥cmc, all the dye molecules are compartmentalized into the micelles in monomeric form and protected from proton transfer quenching relative to that observed in the bulk water [12, 13]. The

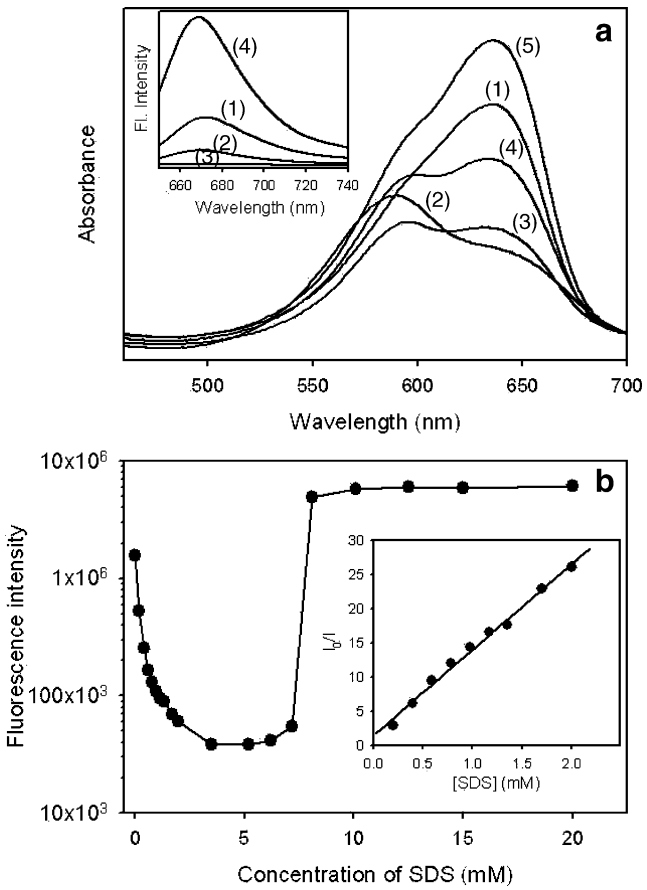

Fig. 1 **a** Absorption spectra of NB in aqueous solution of SDS of varying concentrations, (*1*) 0, (*2*) 3.5, (*3*) 6.0, (*4*) 7.0 and (*5*) 8.0 mM. Fluorescence spectra of NB in aqueous solution of SDS of varying concentrations of (*1*) 0, (*2*) 2.5, (*3*) 5.0, (*4*) 8.0 mM is presented in the inset. **b** Fluorescence intensity of NB (at the peak emission) as a function of SDS concentration. Stern Volmer plot of NB in SDS solutions is presented in the inset. The *straight line* indicates a least-square fitting

huge increase in intensity accompanied by a blue shift is indicative of a probable location of the probe in the nonpolar core region of the micelles with the hydrophobic moiety of the probe intruded into the hydrocarbon core region of the micelle. To verify the huge increase in NB emission intensity as a result of its probable location in the micellar nonpolar interior, we have checked the emission of 2μM NB in dioxane (a less polar solvent compared to water) and found that the emission intensity in dioxane is much higher compared to that in water.

The fluorescence decay pattern of NB in aqueous solution at different concentrations of SDS (using a 633nm diode laser) is shown in Fig. 2. It is found that NB in water shows a single exponential decay with a time constant of 0.34ns, which is comparable to that obtained in earlier studies [15]. It could be noted that NB has a longer excited-state lifetime in nonpolar solvents (of the order of several nanoseconds), and the excited-state lifetime in water is highly quenched due to ultrafast proton transfer [12, 13] resulting in a shorter lifetime. At pre-micellar concentrations of SDS, the excited-state lifetime is reduced further (fitted biexponentially with time constants of 0.29ns (91%) and 0.97ns (9%)) in presence of 2.5mM SDS confirming the quenching. The presence of a long time component in the pre-micellar concentration region might be due to the formation of pre-micellar surfactant aggregate with solubilized dye content as has been reported earlier [25, 26]. However, at [SDS]> cmc, the excited-state lifetime becomes longer (1.2ns, 73%) indicating the residence of the dye in a protective restricted environment of the micellar hydrophobic core. Such a long lifetime of NB in SDS micelles has been reported earlier [27]. Anisotropy of NB in the absence and presence of 50mM SDS has been depicted in the inset of Fig. 2. The rotational reorientation time of the probe in water is found to be 0.16ns, which is consistent with earlier report [15]. In the presence of 50mM SDS a slow component of 0.93ns (60%) is observed along with a fast component of 70ps. The fast component represents the wobbling motion of the dye. The presence of a slow component is consistent with previous result [27] confirming the restricted motion of the dye in the micellar environments [28].

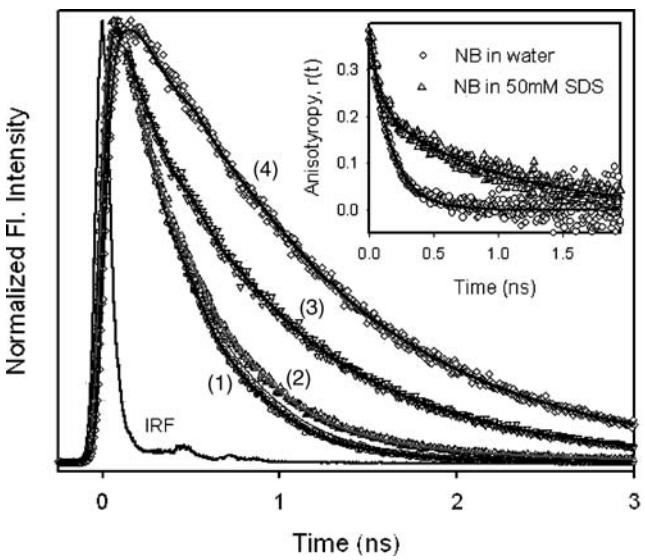

Fig. 2 Picosecond resolved fluorescence transients of NB in absence and presence of various concentrations of SDS solution, (*1*) 0, (*2*) 3.0, (*3*) 8.0 and (*4*) 50.0 mM. Time resolved anisotropy of NB in water and 50 mM SDS is presented in the inset

The effect of caging of NB into the nanoenvironment of AOT RM of different levels of hydration (w_0) on the absorption and emission spectra is shown in Fig. 3a,b. The absorption spectrum at $w_0 = 0$ produces a maximum at 605nm (Fig. 3a). A small hump in the 500nm region indicates the presence of the neutral species [9]. The hump is not prominent due to the presence of trace amount of water in AOT RM even at $w_0 = 0$, which is enough to produce the protonated species. Previously Das et al. [9] have reported an absorption peak at 493nm for the TX-100 RM at $w_0 = 0$. With increasing water content in the RM, absorption maximum suffers a red shift with a peak at 630nm for $w_0 = 20$. The corresponding fluorescence spectra are shown in Fig. 3b. A peak is observed at 643nm for the $w_0 = 0$ RM. With increasing water content of the RM, the fluorescence peak gets red shifted. The red shift of both absorption and fluorescence maxima with increasing w_0 corresponds to the exposure of the dye to more polar environment as w_0 increases. The fluorescence decay transients of the dye at the peak positions in $w_0 = 0$ and $w_0 = 5$ RMs (measured with a 409nm diode laser) are depicted in Fig. 3c and d respectively. It can be seen that for the $w_0 = 0$ RM, the decay transient is relatively slow (with components of 1.25ns, 10% and 3.0ns, 90%) compared to the $w_0 = 5$ RM (with components of 0.38ns, 7% and 1.6ns, 93%). The presence of slow component in the $w_0 = 0$ RM confirms the presence of the unquenched neutral species of NB, whereas the presence of a fast component in the $w_0 = 5$ RM confirms the existence of the protonated species. The slower component being the major one indicates that the motion of the dye is highly restricted inside the RM waterpool and the restriction is progressively released with increasing water content beyond $w_0 = 5$. The time constants do not change appreciably when RM is hydrated further ($w_0 \geq 10$) (The excited state lifetime of NB in $w_0 = 10$ system is 0.37ns (8%) and 1.4ns (92%) and that of $w_0 = 20$ system is 0.33ns (8%) and 1.3ns (92%)). It could be noted that at and beyond $w_0 = 10$, a well-defined water-pool is formed in AOT-RM, in which the entrapped water behaves like bulk water [29–32]. If water is further added into it, no change in the physical property of entrapped water occurs.

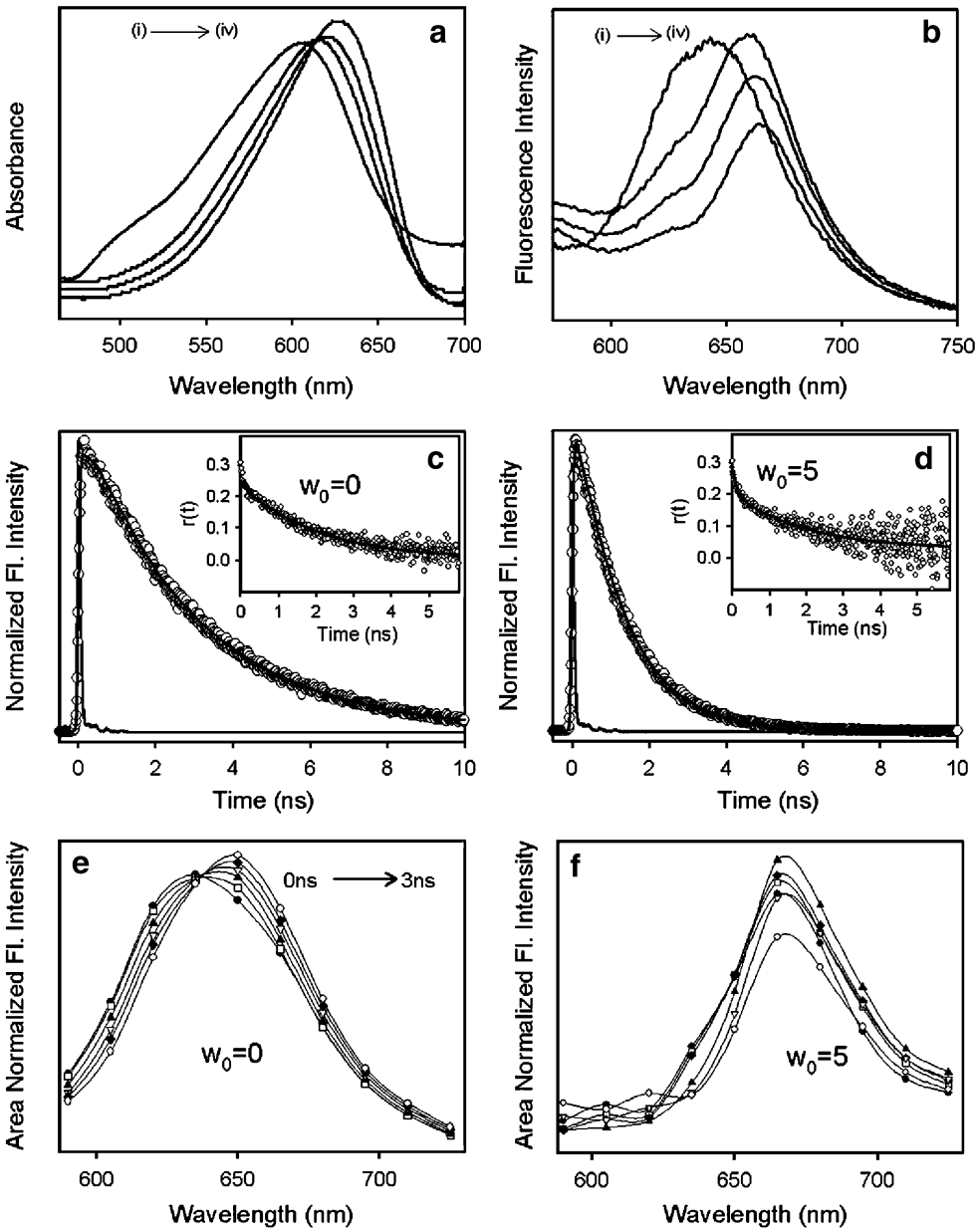

Fig. 3 **a** Absorbance spectra of NB in AOT-RM of varying w_0 values, (*1*) 0, (*2*) 2.5, (*3*) 5, (*4*) 10. **b** Emission spectra of NB in AOT-RM of varying w_0 values, (*1*) 0, (*2*) 2.5, (*3*) 5, (*4*) 10. **c** Picosecond resolved fluorescence transient of NB in AOT-RM with w_0=0. The corresponding anisotropy is presented in the inset. **d** Picosecond resolved fluorescence transient of NB in AOT-RM with w_0=5. The corresponding anisotropy is presented in the inset. **e** TRANES for NB encapsulated in AOT-RM with w_0=0. **f** TRANES for NB encapsulated in AOT-RM with w_0=5

In the present system also, the emission maximum (~666nm) in hydrated RM ($w_0 \geq 10$) is in close agreement with that of NB in pure water (~674nm) and also the average lifetime does not change significantly at $w_0 \geq 10$. It could also be noted that the faster component obtained in hydrated RM systems resembles the excited state lifetime of NB in pure water, which confirms the presence of bulk-like water. However, the longer component stands for the restricted environment. The rotational fluorescence anisotropy of these two RM systems has been depicted in the inset of the respective Fig. 3c and d. As evidenced from the figures, the rotational time constants are slower (0.07ns, 20% and 2.2ns, 80% for the w_0 = 0 RM; 0.1ns, 37% and 2.1ns, 63% for the w_0 = 5 RM) compared to that in pure water. Such a slower anisotropy of the dye is representative of its encagement in the AOT-RM waterpool.

We construct the TRES to determine the nature of solvation of NB in AOT-RM at different w_0 values of 0, 1.25, 2.5 and 5. In none of the studied w_0 values, we found any emission shift, which indicates the absence of solvation [33] in the RM. Perhaps the ultrafast solvation of the present probe in water is beyond the resolution of our experimental setup. To ascertain the possible existence of two kinds of species in the nanocage of AOT, we use the TRANES technique at four different w_0 values of 0, 1.25, 2.5 and 5. The TRANES profiles of two representative systems (w_0 = 0 and w_0 = 5) has been presented in Fig. 3e and f respectively. As evidenced from Fig. 3e, two peaks at

~650nm and ~628nm with a distinct isoemissive point at ~638nm are present in the $w_0 = 0$ RM. The presence of this isoemissive point clearly indicates the existence of two species, one cationic and the other neutral, within the nanocage of AOT-RM. We deconvolute the spectrum at t = 0ns into two spectra peaking at ~666nm (fluorescence peak of NB in hydrated AOT RM) and ~625nm (fluorescence peak of the deprotonated NB [9], and found that the area of the latter is order of magnitude larger than the former confirming the presence of the neutral species at t = 0ns. On the other hand, deconvolution of the spectra at t = 3ns produces larger area for the protonated species confirming its presence in the system. When w_0 is increased to 1.25, the peak in the high-energy region disappears producing only a shoulder, enhancing the peak in the low energy region at ~666nm (resembling the fluorescence peak of highly hydrated AOT RM) with an isoemissive point at ~653nm. The disappearance of the peak in the high-energy region indicates the disappearance of the neutral species with the addition of water and emergence of the protonated species. Red shift of the isoemissive point is also consistent with the argument. With increasing water loading in the RM system, only one peak emerges and no isoemissive point is obtained (Fig. 3f). This indicates the presence of only cationic NB at high w_0. From these studies we confirm that the emission of the probe NB in the aqueous micellar and DNA environments (see below) is only due to a single cationic species.

Figure 4a depicts the absorption spectra of NB in water in the absence and presence of SS-DNA of varying

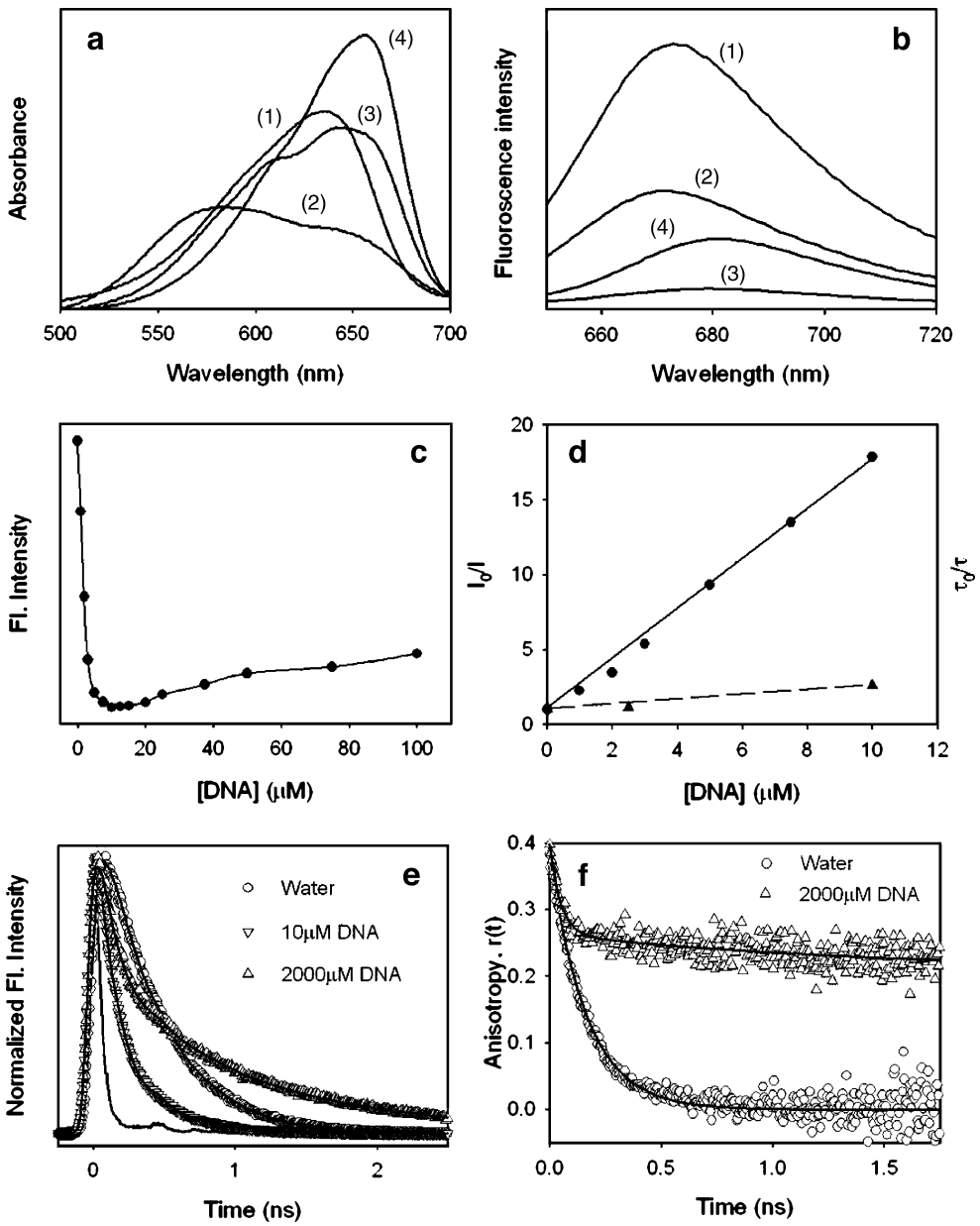

Fig. 4 **a** Absorption spectra of NB in water in absence and presence of a genomic DNA from Salmon sperm of various concentrations, (*1*) 0, (*2*) 5, (*3*) 20, (*4*) 100 μM. **b** Emission spectra of NB in water in absence and presence of various concentrations of a genomic DNA from Salmon sperm of various concentrations, (*1*) 0, (*2*) 2, (*3*) 20, (*4*) 100 μM. **c** Fluorescence intensity of NB (at the peak emission) vs. DNA concentration profile. **d** Stern Volmer plot of NB in DNA. *Circles* represent steady state data (I_0/I) and *triangles* represent time resolved data (τ_0/τ). **e** Picosecond resolved fluorescence transients of NB in absence and presence of various concentrations of DNA. **f** Time resolved anisotropy, of NB in water and in 200 μM DNA

concentrations. When DNA is added into the aqueous solution of NB ([DNA] = 2μM), λ_{max} (=633nm) is marginally blue shifted compared to the aqueous solution accompanied by a considerable decrease in the absorbance. At 5μM DNA, a shoulder at ~570nm develops and on further increase in the DNA concentration to 20μM, the peak at 570nm is red shifted to 605nm with a strengthening of the peak at 640nm. When the concentration of DNA is increased to 100μM, a sharp peak at 655nm appears with higher absorbance than that in the aqueous solution. The appearance of a new peak in the blue region of the spectrum signifies the possibility of the formation of a ligand-DNA complex in the ground state as observed in the NB-SDS system (Fig. 1a). Previously Huang et al. [7] have reported the formation of a complex between NB-sulfate and DNA with a binding constant of 3×10^3l mol^{-1}. From Fig. 4b it is evidenced that the fluorescence intensity reduces considerably at [DNA] = 2μM with no change in the peak position. At 20μM DNA, fluorescence is significantly quenched and the peak has a little red shift to 675nm. However, at 100μM DNA, the intensity of NB fluorescence increases compared to that of 20μM DNA, with a considerable red shift of the peak position (680nm). The fluorescence intensity of NB is plotted against DNA concentration in Fig. 4c. It is found that initially intensity decreases by an order of magnitude with increasing concentration of DNA, and beyond a threshold DNA concentration of 12.5μM, intensity increases. A good linear Stern–Volmer fit is obtained in the quenching regime (Fig. 4d) with K_{SV} of 1.6×10^6l mol^{-1}, which is in the same order of magnitude as reported by Chen et al. (3.2×10^6l mol^{-1} at 20 °C) [1]. We also plot the ratios of excited-state lifetime of the probe in the absence and presence of the DNA (τ_0/τ) against DNA concentration and found that the slope of τ_0/τ is significantly different than that of the corresponding I_0/I, indicating the static nature of the quenching [24] as observed in the case of SDS micelles. Appearance of a new peak in the absorption spectrum (Fig. 4a) with the increase in DNA concentration is also consistent with the formation of ground-state complex, revealing the static nature of the quenching of NB emission.

The nature of the fluorescence quenching of NB upon complexation with the SS-DNA clearly indicates that up to 12.5μM DNA concentration the nature of binding is different from that at higher DNA concentrations. For other cationic intercalators it has been shown earlier that at low DNA concentration, the probe molecules undergo electrostatic binding (non specific) and at higher DNA concentration the probes intercalate into the DNA as the ligand-DNA binding constant is low at low DNA concentration prevailing the electrostatic interaction as the major one, whereas at higher DNA concentration the binding constant increases significantly leading to intercalation [34–36]. From CD experiment, we have confirmed that no ψ form [36] of DNA is formed at this high DNA concentration. For the intercalator ethidium bromide (EB), it is found that the probe changes its mode of interaction with DNA from electrostatic to intercalative at [EB]:[DNA] = 1:6 [36]. It can be argued that the quenching of fluorescence of NB in the low concentration region (up to 10μM DNA) is due to the formation of ligand-DNA complex in the ground state, an effect resembling the quenching of fluorescence by heavy anions through electrostatic interaction [37, 38]. The formation of such a complex is associated with a charge-transfer mechanism, which contributes to the quenching process. The intermediate complex might also facilitate the intersystem crossing (ISC) to the triplet state of the acceptor [39]. It can be noted that the K_{SV} value obtained with SDS-NB pair is smaller than that of the DNA-NB system. The formation of a ligand-SDS (or DNA) complex is a consequence of close approach and fruitful collision of the reacting species. It has been reported earlier that collision between a heavy and a small particle is more probable than those between equal sized particles [40], which signifies the lower K_{SV} value in SDS below cmc compared to that in the DNA. The release of quenching at a higher DNA concentration can be correlated with the intercalation of the ligand within the base pairs of DNA. A detailed study in this aspect involving DNAs of known sequences will be published elsewhere.

Figure 4e shows the fluorescence decay transients (measured using a 633nm diode laser) of NB in water in the absence and presence of DNA. At 2.5μM DNA, the fluorescence transient shows biexponential decay with time constants of 0.29ns (95%) and 0.74ns (5%). On further increase of DNA concentration to 10μM, the overall fluorescence transient becomes faster (0.13ns (92%) and 1.0ns (8%)). Note that at this DNA concentration, NB suffers significant quenching (Fig. 4b) due to electrostatic binding to the DNA. At an elevated DNA concentration of 200μM, the slower component (1.2ns, 73%) becomes the major one with a fast component of 0.18ns (27%). When the concentration of the DNA is increased to 2,000μM, the slower component remains the major one. The overall slow decay of the probe in the presence of high concentration of DNA confirms its residence in the protected region of the DNA by intercalative nature of binding. The corresponding picosecond resolved fluorescence anisotropy of the probe in water and 200μM DNA are shown in Fig. 4f. The presence of a fast component (135ps, 35%) of rotational anisotropy in 200μM DNA indicates the existence of a weakly bound NB at the DNA surface and/or wobbling dynamics of the probe NB at the site of intercalation [41]. The presence of a considerably high offset value (66%) in the temporal fluorescence anisotropy decay is consistent with intercalative binding of NB inside the base pairs, which essentially reveals the global motion of the DNA [41].

To compare the binding nature of NB with DNA and SDS, we carry out steady state and time resolved fluorescence study of NB in the presence of both DNA and SDS. Figure 5a depicts the relative change of fluorescence intensity of NB (a Stern–Volmer type of plot) as a function of SDS concentration in the presence of fixed amounts of DNA (2, 50 and 200 μM). A linear fit is obtained when [DNA]:[NB] ratio is low (1:1), with the corresponding quenching constant of 4.6×10^3 l mol^{-1}. This value is expectedly smaller than that obtained in free SDS in water (1.3×10^4 l mol^{-1}). At this low concentration of DNA, most of the NB molecules could be assumed to be electrostatically bound to the DNA surface and being further quenched by SDS monomers. With high values of DNA concentrations, however, no significant quenching of NB fluorescence is obtained. It is found that with 50 μM DNA, only a marginal quenching occurs beyond an SDS concentration of 1 mM, whereas for a higher concentration of DNA (200 μM), the quenching occurs only beyond 2 mM SDS (inset of Fig. 5a). This result suggests that at higher DNA concentration, most of the NB molecules are strongly intercalated within the DNA, however, there is always a possibility that a small fraction of NB is electrostatically bound to the DNA surface, which is also evident from the anisotropy study (Fig. 4f). These results also indicate that with increasing DNA concentration, the

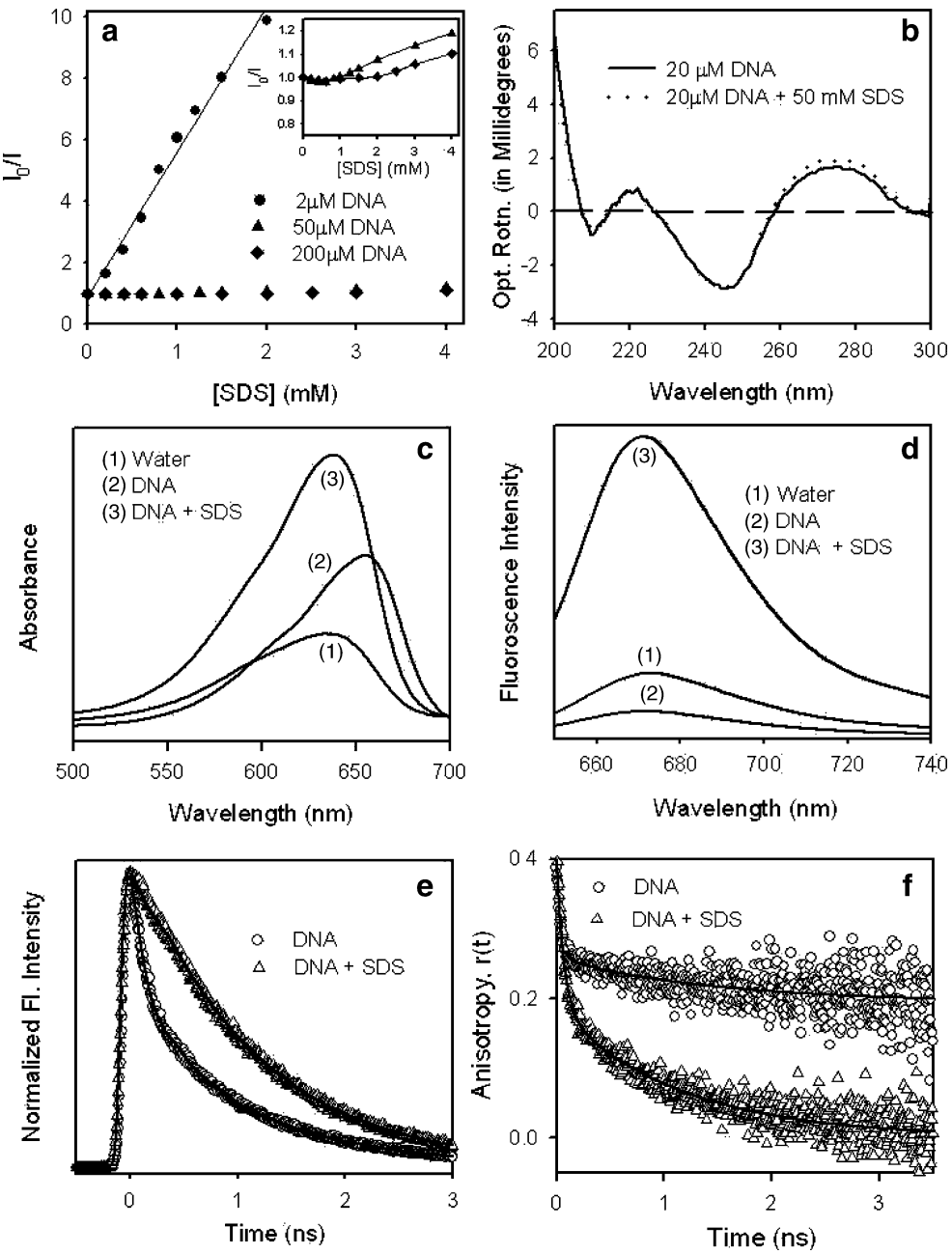

Fig. 5 **a** Stern Volmer plot of NB in SDS solutions in presence of various concentrations of DNA. The *solid line* represents a least-square fitting. The plot for higher SDS concentrations is presented in the inset. The *solid lines* are guide for the eyes. **b** CD spectra of 20 μM DNA in absence and presence of 50 mM SDS. **c** Absorption spectra of 2000 μM DNA in absence and presence of 50 mM SDS. **d** Emission spectra of 2000 μM DNA in absence and presence of 50 mM SDS. **e** Picosecond resolved fluorescence transients of NB in 2000 μM DNA in absence and presence of 50 mM SDS. **f** Time resolved anisotropy of NB in 2000 μM DNA in absence and presence of 50 mM SDS

fraction of electrostatically bound NB decreases as more and more probe molecules are intercalated in the DNA. It should be noted that DNA surface and the head group of SDS are negatively charged. So a close approach of SDS and DNA is energetically forbidden. CD spectrum of the SS DNA in the absence and presence of SDS has been shown in Fig. 5b. The CD spectra of SS DNA resembles that of the physiologically relevant B-form of DNA [36]. Addition of SDS does not perturb the native B-form of the DNA indicating that SDS does not interact strongly with the DNA. However, as the concentration of SDS is increased, such proximity becomes probable due the diffusion of SDS molecules. Thus quenching in the present study commences only beyond a threshold concentration of SDS. The dependence of NB fluorescence intensity on the DNA concentration in the presence of 50 mM SDS is also studied. It is observed that fluorescence intensity remains almost unaltered as a function of DNA concentration, indicating that at such a high concentration of SDS, the dye prefers to reside in a protected micellar environment than in the DNA.

The effect of SDS micelles on the DNA-binding of NB at much higher DNA concentration ([DNA]=2000 μM) is shown in Fig. 5c. As evident from the figure, in the presence of DNA a red shift of the absorption maximum occurs along with an increase in the absorbance. Upon addition of 50 mM SDS, the peak coincides with that of water with an increase of absorbance. A similar trend is observed in the emission spectra (Fig. 5d). It can be observed that the fluorescence intensity of NB increases many fold as SDS micelles are added in the DNA solution. The probe moves from the DNA interior to the hydrophobic core of SDS micelles wherein its intensity increases rapidly. It could be noted that the quenching suffered by the probe in the DNA is relived in the micellar interior, which in turn also increases the emission intensity. The corresponding time-resolved study is presented in Fig. 5e. It can be observed that the decay pattern of NB in DNA consists of a fast component (0.27 ns, 20%) along with a slow component of 1.22 ns (80%) as the major one. In the presence of 50 mM SDS, the contributions of the fast components become insignificant (3%) with a slow component of 1.3 ns as the major one, identical to that of an SDS micellar system. A similar conclusion can be drawn from the anisotropy study (Fig. 5f) wherein a similar timescale of rotational reorientation (70 ps (45%) and 1.1 ns (55%)) has been observed for the DNA + SDS system. The results clearly indicate a migration of the dye NB from DNA to micellar environment.

The exclusion of the intercalated dye from the DNA by SDS micelles is interesting because DNA and SDS micelles are supposed to be non-interacting owing to their similar surface charge. It could be noted that the intercalation process of a small ligand into the base pairs of DNA is a dynamical equilibrium process in which ligand monomer is in equilibrium with the intercalated ligand [42]. The present study shows that in the presence of SDS micelles, the equilibrium process is shifted toward the dissociation of intercalated NB monomers from the DNA. This result infers that in order to affect the rate of dissociation of NB from DNA, the SDS micelles have to bind or at least have to get very close to the negatively charged DNA surface. However, the presence of aromatic ring systems in combination with positive charge of NB may attract the negatively charged SDS micellar surface [43]. The hydrophobic environment of SDS micelles might also cause transient fluctuation in otherwise quite compact DNA duplex structure. This might provide a safer residence to the hydrophobic moiety of the intercalated ligands. A detailed thermodynamic study of the intercalated NB-DNA dissociation and free NB-SDS micelle association is of potential importance and is underway in our laboratory.

Conclusions

In this report we explore the nature of binding interaction of a fluorescent dye/drug Nile blue (NB) with SDS micelles and a genomic DNA. Picosecond resolved fluorescence quenching and polarization analyzed anisotropy of NB in the DNA clearly reveal the interaction of the probe with the DNA molecules. Our studies depict two types of binding modes of the probe drug with DNA; non-specific electrostatic at lower [DNA]:[NB] ratios and intercalative at the higher DNA concentration in the solution. Emission of NB is quenched by low concentration of DNA (through electrostatic interaction) and quenching is partially released in the presence of high concentration of DNA (through intercalative interaction). The nature of the binding of NB in the presence of the DNA and SDS micelles reveals more stable NB-micelle complexation compared to that with the DNA. CD study confirms the structural integrity of the DNA in the presence of micelles. Our studies would help in effectively using the non-toxic DNA-binding drug NB as an efficient DNA probe.

Acknowledgement We thank DST for financial grant (SR/FTP/PS-05/2004).

References

1. Chen Q, Li D, Yang H, Zhu Q, Xu J, Zhao Y (1999) Interaction of a novel red-region fluorescent probe, Nile blue, with DNA and its application to nucleic acids assay. Analyst 124:901–907
2. van Staveren HJ, Speelman OC, Witjes MJH, Cincotta L, Star WM (2001) Fluorescence imaging and spectroscopy of ethyl Nile

blue A in animal models of (pre)malignancies. Photochem Photobiol 73:32–38
3. Morgan J, Potter WR, Oseroff AR (2000) Comparison of photodynamic targets in a carcinoma cell line and its mitochondrial DNA-deficient derivative. Photochem Photobiol 71:747–757
4. Singh G, Espiritu M, Shen XY, Hanlon JG, Rainbow AJ (2001) In vitro induction of PDT resistance in HT29, HT1376 and SK-N-MC cells by various photosensitizers. Photochem Photobiol 73:651–656
5. Huang CZ, Li YF, Hu XL, Li NB (1999) Three-dimensional spectra of the long-range assembly of Nile blue sulfate on the molecular surface of DNA and determination of DNA by light-scattering. Anal Chim Acta 395:187–197
6. Ju H, Ye Y, Zhu Y (2005) Interaction between Nile blue and immobilized single- or double-stranded DNA and its application in electrochemical recognition. Electrochim Acta 50:1361–1367
7. Huang CZ, Li YF, Zhang DJ, Ao XP (1999) Spectrophotometric study on the supramolecular interactions of Nile blue sulphate with nucleic acids. Talanta 49:495–503
8. Yang Y, Hong HY, Lee IS, Bai DG, Yoo GS, Choi JK (2000) Detection of DNA using a visible dye, Nile blue, in electrophoresed gels. Anal Biochem 280:322–324
9. Das K, Jain B, Patel HS (2004) Nile blue in triton-X 100/benzene–hexane reverse micelles: a fluorescence spectroscopic study. Spectrochim Acta, Part A: Mol Biomol Spectrosc 60:2059–2064
10. Hong-Wen G, Qing-Song Y, Liu WG (2002) Langmuir aggregation of Nile blue and safranine T on sodium dodecylbenzenesulfonate surface and its application to quantitative determination of anionic detergent. Anal Sci 18:455–459
11. Kobayashi T, Takagi Y, Kandori H, Kemnitz K, Yoshihara K (1991) Femtosecond intermolecular electron transfer in diffusionless, weakly polar systems: nile blue in aniline and *N*,*N*-dimethylaniline. Chem Phys Lett 180:416–422
12. Douhal A (1994) Photophysics of Nile blue A in proton-accepting and electron-donating solvents. J Phys Chem 98:13131–13137
13. Grofcsik A, Kubinyi M, Jones WJ (1996) Intermolecular photoinduced proton transfer in Nile blue and oxazine 720. Chem Phys Lett 250:261–265
14. Kubinyi M, Brátán J, Grofcsik A, Biczók L, Poór B, Bitter I, Grün A, Bogáti B, Tóth K (2002) Proton transfer and supramolecular complex formation between Nile blue and tetraundecylcalix[4] resorcinarene—a fluorescence spectroscopic study. J Chem Soc, Perkin Trans 2:1784–1789
15. Dutt GB, Doraiswamy S, Periasamy N, Venkataraman B (1990) Rotational reorientation dynamics of polar dye molecular probes by picosecond laser spectroscopic technique. J Chem Phys 93:8498–8513
16. Gallagher SR (1994) In: Ausubel FM, Brent R, Kingston KE, Moore DD, Seidman JG, Smith JA, Struhl K (eds) In current protocols in molecular biology. Greene and Wiley-Interscience, New York
17. Mitra RK, Sinha SS, Pal SK (2007) Temperature dependent hydration at micellar surface: activation energy barrier crossing model revisited. J Phys Chem B 111:7577–7581
18. Periasamy N, Koti ASR (2003) Time resolved fluorescence spectroscopy: TRES and TRANES. Proc Indian Natn Sci Acad 69A:41–48
19. Koti ASR, Krishna MMG, Periasamy N (2001) Time-resolved area-normalized emission spectroscopy (TRANES): a novel method for confirming emission from two excited states. J Phys Chem A 105:1767–1771
20. Koti ASR, Periasamy N (2001) TRANES analysis of the fluorescence of Nile red in organized molecular assemblies confirms emission from two species. Proc Indian Natn Sci Acad (Chem Sci) 113:157–163
21. O'Connor DV, Philips D (1984) Time correlated single photon counting. Academic, London
22. Sarkar M, Poddar S (2000) Studies on the interaction of surfactants with cationic dye by absorption spectroscopy. J Colloid Interface Sci 221:181–185
23. Pal P, Zeng H, Durocher G, Girard D, Giasson R, Blanchard L, Gaboury L, Villeneuve L (1996) Spectroscopic and photophysical properties of some new rhodamine derivatives in cationic, anionic and neutral micelles. J Photochem Photobiol A, Chem 98:65–72
24. Lakowicz JR (1999) Principles of fluorescence spectroscopy. Kluwer, New York
25. Diaz Garcia ME, Sanz-Medel A (1986) Dye-surfactant interactions: a review. Talanta 33:255–264
26. Neumann MG, Gehlen MH (1990) The interaction of cationic dyes with anionic surfactants in the premicellar region. J Colloid Interface Sci 135:209–217
27. Romani AP, Gehlen MH, Lima GAR, Quina FH (2001) The change in the properties of sodium dodecyl sulfate micelles upon addition of isomeric and unsaturated short-chain alcohols probed by photophysical methods. J Colloid Interface Sci 240:335–339
28. Shaw AK, Pal SK (2007) Activity of subtilisin Carlsberg in macromolecular crowding. J Photochem Photobiol B 86:199–206
29. Goto A, Harada S, Fujita T, Miwa Y, Yoshioka H, Kishimoto H (1993) Enthalpic studies on the state of water in sodium bis(2-ethylhexyl)sulfosuccinate reversed micelles. Langmuir 9:86–89
30. Goto A, Yoshioka H, Kishimoto H, Fujita T (1992) Calorimetric studies on the state of water in reversed micelles of sodium bis(2-ethylhexyl)sulfosuccinate in various solvents. Langmuir 8:441–445
31. Belletete M, Lachapelle M, Durocher G (1990) Dynamics of interfacial interactions between the molecular probe 2-(p-(dimethylamino)phenyl)-3,3-dimethyl-3H-indole and the aerosol OT inverted micelles. J Phys Chem 94:7642–7648
32. Correa NM, Biasutti MA, Silber JJ (1995) Micropolarity of reverse micelles of aerosol-OT in *n*-hexane. J Colloid Interface Sci 172:71–76
33. Horng ML, Gardecki JA, Papazyan A, Maroncelli M (1995) Subpicosecond measurements of polar solvation dynamics: coumarin 153 revisited. J Phys Chem 99:17311–17337
34. McMurray CT, Small EW, Van Holde KE (1991) Binding of ethidium to the nucleosome core particle. 2. Internal and external binding modes. Biochemistry 30:5644–5652
35. McMurray CT, Van Holde KE (1991) Binding of ethidium to the nucleosome core particle. 1. Binding and dissociation reactions. Biochemistry 30:5631–5643
36. Sarkar R, Pal SK (2006) Ligand-DNA interaction in a nanocage of reverse micelle. Biopolymers 83:675–686
37. Bortolus P, Bartocci G, Mazzucato U (1975) Excited state reactivity of aza aromatics. III. Quenching of fluorescence and photoisomerization of azastilbenes by inorganic anions. J Phys Chem 79:21–25
38. Watkins AR (1973) Quenching of biphenyl fluorescence by inorganic ions. J Phys Chem 77:1207–1210
39. Atherton SJ, Beaumont PC (1987) Laser flash photolysis of DNA-intercalated ethidium bromide in the presence of methylviologen. J Phys Chem 91:3993–3997
40. Heller W, Rowe E, Berg R, Watson JHL (1959) Effect of partial coagulation upon the size distribution curve in heterodisperse colloidal systems. J Phys Chem 63:1566–1569
41. Millar DP, Robbins RJ, Zewail AH (1982) Torsion and bending of nucleic acids studied by subnanosecond time-resolved fluorescence depolarization of intercalated dyes. J Chem Phys 76:2080–2094
42. Wilhelmsson LM, Westerlund F, Lincoln P, Norden B (2002) DNA-binding of semirigid binuclear ruthenium complex,-[-(11,11′-bidppz)(phen)4Ru2]4+: extremely slow intercalation kinetics. J Am Chem Soc 124:12092–12093
43. Westerlund F, Wilhelmsson LM, Norden B, Lincoln P (2003) Micelle-sequestered dissociation of cationic DNA-intercalated drugs: unexpected surfactant-induced rate enhancement. J Am Chem Soc 125:3773–3779